Biochimica et Biophysica Acta 1808 (2011) 752–760

Contents lists available at ScienceDirect

Biochimica et Biophysica Acta

journal homepage: www.elsevier.com/locate/bbamem

Plant pentacyclic triterpenic acids as modulators of lipid membrane physical properties

Jesús Prades [a,1], Oliver Vögler [a,1], Regina Alemany [a], Manuel Gomez-Florit [a], Sérgio S. Funari [b], Valentina Ruiz-Gutiérrez [c], Francisca Barceló [a,*]

[a] Clinical and Translational Research Group, IUNICS, University of the Balearic Islands, E-07122 Palma de Mallorca, Spain
[b] HASYLAB, Notkestrasse 85, D-22603 Hamburg, Germany
[c] Nutrition and Lipid Metabolism, Instituto de la Grasa, Consejo Superior de Investigaciones Científicas (CSIC), E-41012 Sevilla, Spain

ARTICLE INFO

Article history:
Received 27 September 2010
Received in revised form 22 November 2010
Accepted 9 December 2010
Available online 15 December 2010

Keywords:
Plant triterpenic acid
Triterpene–membrane interaction
Membrane structure

ABSTRACT

Free triterpenic acids (TTPs) present in plants are bioactive compounds exhibiting multiple nutriceutical activities. The underlying molecular mechanisms have only been examined in part and mainly focused on anti-inflammatory properties, cancer and cardiovascular diseases, in all of which TTPs frequently affect membrane-related proteins. Based on the structural characteristics of TTPs, we assume that their effect on biophysical properties of cell membranes could play a role for their biological activity. In this context, our study is focused on the compounds, oleanolic (3β-hydroxy-12-oleanen-28-oic acid, OLA), maslinic (2α,3β-dihydroxy-12-oleanen-28-oic acid, MSL) and ursolic ((3β)-3-hydroxyurs-12-en-28-oic acid, URL) as the most important TTPs present in *orujo olive oil*. X-ray diffraction, differential scanning calorimetry, ^{31}P nuclear magnetic resonance and Laurdan fluorescence data provide experimental evidence that OLA, MSL and URL altered the structural properties of 1,2-dipalmitoyl-*sn*-glycero-3-phosphatidylcholine (DPPC) and DPPC-Cholesterol (Cho) rich membranes, being located into the polar-hydrophobic interphase. Specifically, in DPPC membranes, TTPs altered the structural order of the $L_{\beta'}$, phase without destabilizing the lipid bilayer. The existence of a nonbilayer isotropic phase in coexistence with the liquid crystalline L_α phase, as observed in DPPC:URL samples, indicated the presence of lipid structures with high curvature (probably inverted micelles). In DPPC:Cho membranes, TTPs affected the membrane phase properties increasing the Laurdan GP values above 40 °C. MSL and URL induced segregation of Cho within the bilayer, in contrast to OLA, that reduced the structural organization of the membrane. These results strengthen the relevance of TTP interactions with cell membranes as a molecular mechanism underlying their broad spectrum of biological effects.

1. Introduction

Pentacyclic triterpenes present in plants exist in the free acid form or as aglycones in triterpenoid saponins. Among the free triterpenic acids (TTPs), oleanolic (3β-hydroxy-12-oleanen-28-oic acid, OLA), maslinic (2α,3β-dihydroxy-12-oleanen-28-oic acid, MSL) and ursolic acid (3β-hydroxyurs-12-en-28-oic acid, URL) (Fig. 1) are interesting secondary plant products with multiple nutriceutical activities [1,2]. These bioactive compounds constitute a component of the non-glyceride fraction of pomace olive oil, also called *orujo olive oil*, which is consumed in the human mediterranean diet [3,4]. For these reasons there is a growing interest to decipher the details of the molecular mechanisms of the dietary plant triterpenes.

Previous studies have demonstrated that TTPs have anti-inflammatory and antioxidant properties [2,5–9], exert antihypertensive, antihyperlipidemic and anti-diabetic effects in experimental animal models [10–14], possess antiviral activity [15] and show remarkable results in suppressing tumour genesis and inhibiting tumours [16–

Abbreviations: TTP, free triterpenic acid; PL, phospholipids; PC, phosphatidylcholine; DPPC, 1,2-dipalmitoyl-*sn*-glycero-3-phosphatidylcholine; POPC, 1-palmitoyl-2-oleoyl-*sn*-glycero-3-phosphocholine; DEPE, 1,2-dielaidoyl-*sn*-glycero-3-phosphatidylethanolamine; Cho, cholesterol; OLA, oleanolic acid; MSL, maslinic acid; URL, ursolic acid; Laurdan, 6-dodecanoyl-2-(dimethylamino)naphthalene; DPH, 1,6-diphenyl-1,3,5-hexatriene; MLV, multilamellar lipid vesicles; SUV, small unilamellar vesicles; DSC, differential scanning calorimetry; $L_{\beta'}$, gel lamellar phase; $P_{\beta'}$, rippled phase; L_α, liquid-crystalline lamellar phase; H_{II}, inverted hexagonal phase; d, bilayer repeat period; T_p, lamellar gel-to-rippled phase transition temperature; T_m, gel-to-liquid crystalline phase transition temperature; T_H, lamellar-to-inverted hexagonal phase transition temperature; ΔH, enthalpy change

* Corresponding author. Departamento de Biología Fundamental, University of the Balearic Islands, E-07122 Palma de Mallorca, Spain. Tel.: +34 971173149; fax: +34 971173184.
E-mail address: francisca.barcelo@uib.es (F. Barceló).
[1] Both authors contributed equally to the work.

0005-2736/$ – see front matter © 2010 Elsevier B.V. All rights reserved.
doi:10.1016/j.bbamem.2010.12.007

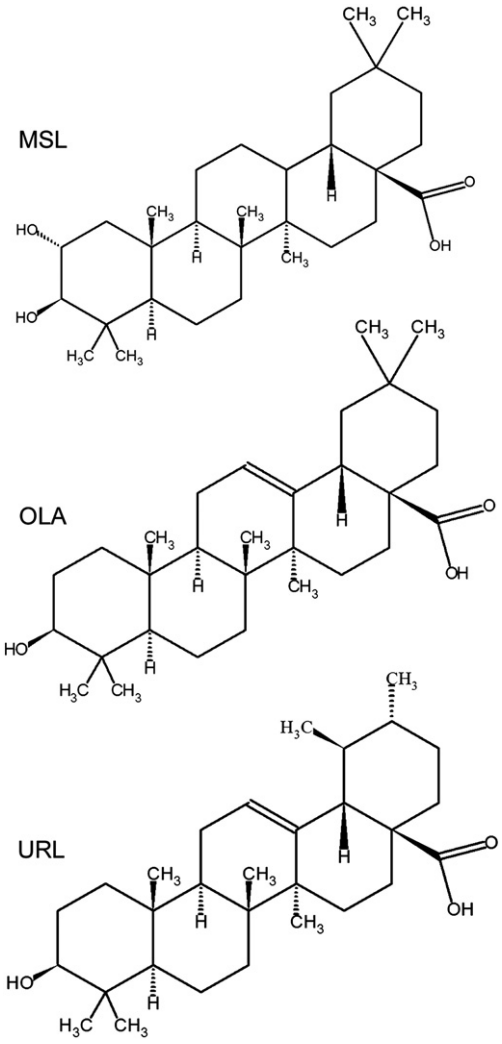

Fig. 1. Chemical structure of the pentacyclic triterpenic acids. Oleanoic (OLA), maslinic (MSL) and ursolic (URL) acid.

20]. Moreover, pentacyclic triterpenes have been reported to have cytotoxic effects on distinct multidrug-resistant leukemic cell lines [21]. However, the molecular mechanisms underlying the diverse TTP activities have only been examined in part. The anti-inflammatory action was related to their capacity to suppress inducible nitric oxide synthethase gene enzyme expression that may occur through suppressed production of pro-inflamatory cytokines [22]. Regarding cardiovascular disease, it has been demonstrated that TTPs present in olive oil and pomace olive oil have vasodilatory activity in isolated artery of both normotensive and spontaneously hypertensive rats [11,12]. In addition, the ingestion of pomace olive oil with a high proportion of OLA attenuated the endothelial dysfunction associated with hypertension [13]. The vasoprotective mechanism of TTPs seems to involve endothelium-dependent release of nitric oxide mediated by the signal transducer enzyme, phosphoinositide-3-kinase [7]. The TTP effect on diet-induced hyperlipidemia has been related to their capacity to inhibit ACAT gene expression that controls the key enzyme regulating plasma fatty acid metabolism [14].

On the other hand, the antitumoral and pro-apoptotic properties were related mainly to the regulating effect of the activity and/or expression of enzymatic systems. These are involved in specific signal transduction pathways that play a role in the extrinsic [23] as well as intrinsic mitochondrial apoptotic pathway induced by ROS generation [17]. A recent biological screening of several natural triterpenoids and synthetic derivatives against G-protein coupled receptor TGR5 has revealed that some TTPs, such as betulinic acid, OLA and URL, presented selective TGR5 agonist activity [24]. Interestingly, the G-protein coupled receptor TGR5 participates in the control of energy metabolism, preventing obesity and insulin resistance, being a special drug target for the treatment of metabolic diseases [25]. Thus, TGR5 agonist activity of TTPs might become a new nutriceutical perspective for these diseases.

One important aspect of the above mentioned molecular mechanisms is the fact that membrane-related processes are frequently an integral part of them [19,24], which is demonstrated by the following examples: i) inflammation and lipid peroxidation are phenomena, which to a large extent take place at the cell-surface, ii) membrane proteins of organelles, such as endoplasmatic reticulum or lysosomes, participate in pro-apoptotic signalling events [26], iii) permeabilization of the mitochondrial membrane is a pivotal step in the apoptotic pathway cascades [27] and iv) the differentiation process of some cell types has been related to alterations in the plasma membrane fluidity [28,29]. Based on these observations, one may hypothesize that part of the molecular mechanism to explain the distinct biological activities of TTPs may be related to a direct effect of this compound class on the cell membrane. Indeed, pentacyclic TTPs have structural similarities to cholesterol, which convert them into good candidates to interact with the biomembranes. It is probable that such interactions would modulate the structural properties of the affected membranes and this may provoke the functional changes of membrane-related proteins. It might also be possible that the above mentioned TTP binding to the G-protein coupled receptor TGR5 [25] could, at least to some degree, be modulated by the structural properties of the lipid bilayer and/or the TTP effects on the cell membrane.

It is rather surprising that only very few studies have explored the effects of TTPs on the phospholipid (PL) membranes and the majority of them deal with the triterpenoid saponins with haemolytic activity [30–32]. Using physico-chemical techniques, the aim of this paper is to analyse the effect of OLA, URL (a positional isomer) and MSL (a hydroxyl-derivative of OLA), as the most important TTPs present in the dietary *orujo olive oil,* on the structural properties of PC and PC-cholesterol rich membranes, in order to provide the first detailed molecular basis of the TTP–membrane interactions.

2. Materials and methods

2.1. Materials

1,2-dipalmitoyl-*sn*-glycero-3-phosphatidylcholine (DPPC), 1-palmitoyl-2-oleoyl-*sn*-glycero-3-phosphocholine (POPC) and 1,2-dielaidoyl-*sn*-glycero-3-phosphatidylethanolamine (DEPE) were purchased from Avanti Polar Lipids, Inc. (Alabaster, U.S.A.) and stored under argon at −80 °C. 2α-hydroxyoleanoic acid (maslinic acid, MSL) from olive oil was kindly provided by Dra. A. Guinda (Instituto de la Grasa, CSIC-Sevilla, Spain). Oleanoic (OLA) and ursolic acid (URL), N-(2-Hydroxy ethyl) piperazine-N′-(2-ethanesulfonic acid) sodium salt (Hepes) and cholesterol (Cho) were obtained from Sigma-Aldrich (Madrid, Spain). 2-dimethylamino-(6-lauroyl)-naphthalene (Laurdan), and 1,6-diphenyl-1,3,5-hexatriene (DPH) from Molecular Probes (Invitrogen, Barcelona, Spain).

2.2. Model membranes and sample preparation

Multilamellar lipid vesicles (MLV; 15% (w/w) were prepared in 10 mM Hepes, 100 mM NaCl, 1 mM EDTA, pH 7.4 (Hepes buffer) for X-ray diffraction experiments, or in D_2O for nuclear magnetic resonance (NMR) analysis, according to established procedures [33]. Lipid powder was hydrated in the presence or absence of the triterpenic acid (TTP), oleanoic (OLA), maslinic (MSL) or ursolic (URL) at the desired molar ratio, and the mixture was thoroughly homogenized with a pestle-type minihomogenizer (Sigma) and by vortexing. The

suspensions were then submitted to five temperature cycles (heating to 70 °C and cooling to −20 °C), stored at 4 °C until use and equilibrated prior to data acquisition.

For DSC experiments, lipid mixtures (5 mg) were dissolved in chloroform and the solvent was evaporated under argon and vacuum-dried. A known weight of lipid sample (~3 mg) was transferred to an aluminum pan and hydrated by adding Hepes buffer to a final concentration of 15% (w/w). The pans were sealed and submitted to ten heating and cooling cycles (70 °C to −20 °C), to ensure complete homogenization before measurements. For fluorescence spectroscopy experiments, lipids and the fluorescence probes Laurdan (lipid:probe, 250:1, mol:mol) or DPH (lipid:probe, 750:1, mol:mol) were dissolved together in chloroform:methanol (2:1, v/v) and the solvent evaporated under argon and vacuum-dried. The lipid film was hydrated with Hepes buffer to a final lipid concentration of 50 μM and the mixtures were submitted to five temperature cycles (70 °C and −20 °C). Small unilamellar vesicles (SUV) were prepared from MLV by sonication in an ice–water bath with a Branson 250 sonicator equipped with a microtip until the solution became clear.

2.3. X-ray diffraction analysis

Small and Wide-Angle Synchrotron radiation X-ray scattering (SAXS and WAXS) data were collected simultaneously, using standard procedures on the Soft Condensed Matter beamline A2 at storage ring Doris III of HASYLAB (DESY, Hamburg, Germany). The samples were fixed in a temperature-controlled sample holder and heated from 25 °C to 50 °C and then cooled-down to 25 °C at a scan rate of 1 °C/min. Samples containing DEPE were heated to 75 °C and then cooled to 25 °C. The data collection conditions were the same as those described previously [33].

2.4. Differential scanning calorimetry (DSC)

Experiments were conducted in a DSC 2920 scanning calorimeter (TA instruments). Samples were run at a scan rate of 5 °C/min in a temperature range of 25–50 °C for DPPC and −10–20 °C for POPC mixtures. To ensure the reproducibility of the results, four scan cycles were recorded for each sample and the fourth heating scan was used to evaluate the thermotropic transitions. After the thermal measurements, the phospholipid content of each sample was quantified by ICP spectrophotometry (Perkin-Elmer Optima 5300 DV). DSC data were analysed with the instrument's software package. The lipid phase transition temperatures (T_p, T_m and T_H) were determined from the maximum of the excess heat flow *vs* the temperature curves and the transition enthalpies were obtained from the area under the peaks. Peak decomposition analysis of the calorimetric peaks was done using mathematical fitting curves (PeakFit v4.12).

2.5. ^{31}P nuclear magnetic resonance (NMR) spectroscopy

Measurements were conducted employing a Bruker Avance-300 multinuclear NMR spectrometer operating at 121.49 MHz using broad-band proton decoupling and 4 mm thin-walled tubes. Free induction decays were obtained from up to 200 transients employing a 4.40 μs 90° radio-frequency pulse, 24.3-kHz spectral width and 64-K data points. The relaxation delay time was 2 s. Data were analysed using Bruker software. The ^{31}P spectra were referenced relative to pure lysophosphatidylcholine micelles (0 ppm). Samples were equilibrated at the working temperatures for 15 min before data acquisition.

2.6. Fluorescence spectroscopy

A Cary Eclipse (FL0902M009, Varian) and a MPF-66 (Perkin-Elmer Ltd.) fluorescence spectrofluorometers were used to monitor the steady-state Laurdan fluorescence emission and the DPH fluorescence polarization, respectively. The temperature was controlled by a circulating water bath. Samples were equilibrated for 5 min at each temperature, prior to measurement. The fluorophore Laurdan was excited at 350 nm and the fluorescence emission spectra were recorded between 380 and 550 nm in the range temperature of 25–50 °C. The interference of scattered light was negligible. Generalised polarization (GP) was calculated from the emission intensities at 435 and 500 nm using the following equation [34]:

$$GP = (I_{435} - I_{500}) / (I_{435} + I_{500})$$

The fluorofore DPH was excited at 360 nm and the emission was registered at 427 nm with a slit width of 2 nm. The scattered light from the excitation source to the measured light at 427 nm was determined using an unlabeled reference lipid solution of the same

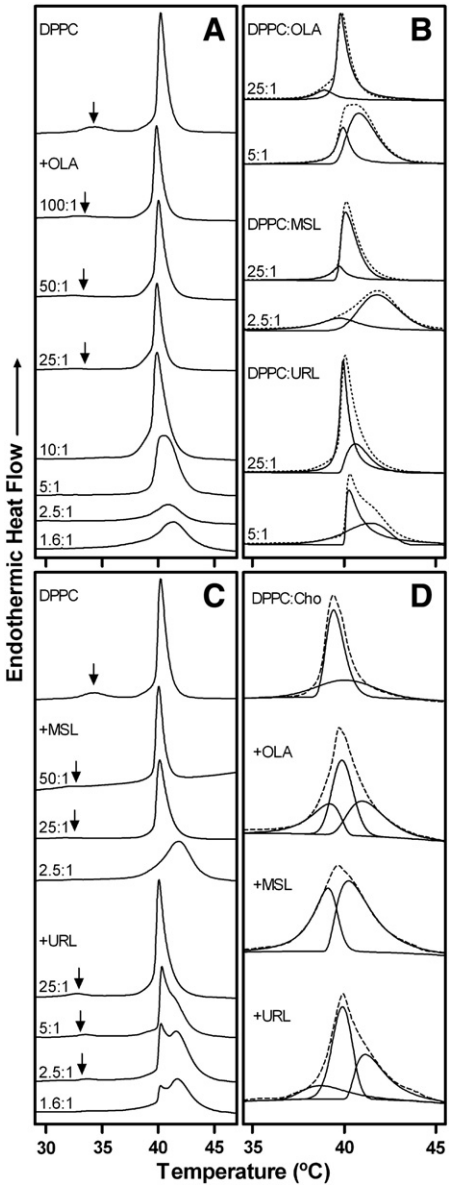

Fig. 2. DSC heating thermograms of DPPC and DPPC-cholesterol rich membranes in presence of triterpenic acids. Dispersions containing (A) DPPC:OLA and (B) DPPC:MSL and DPPC:URL at the molar ratio indicated in each thermogram. Peak decomposition analysis of the calorimetric peak of (C) DPPC:TTP and (D) DPPC:Cho:TTP (70:30:10, lipid molar ratio) mixtures: experimental data (- - -) and individual components (—). Endothermic heat flow was normalised to phospholipid concentration. DSC scans were performed at a scan rate of 5°C/min.

Table 1
Calorimetric data of the effect of triterpenic acids in DPPC and POPC membranes. DPPC, 1,2-dipalmitoyl-*sn*-glycero-3-phosphoethanolcholine; POPC, 1-palmitoyl-2-oleoyl-*sn*-glycero-3-phosphocholine; Cho, cholesterol; OLA, oleanoic acid; MSL, maslinic acid; URL, ursolic acid. The enthalpy values of the $L_{\beta'}$-to-$P_{\beta'}$ and $P_{\beta'}$-to-L_{α} phase transitions correspond to the whole area of the curve. Calorimetric data are mean values of two independent experiments. The transition temperature represents the maximum of the excess heat flow *vs* temperature curves. T_{m1} and T_{m2} are the transition temperatures of the two peaks obtained in the deconvolution analysis of the L_{β}-to-L_{α} transition curve. H_{m1} and H_{m2} are the relative areas of each peak.

Sample	Molar ratio	T_p (°C)	H_p (kcal/mol)	$T_{m(1)}$ (°C)	$T_{m(2)}$ (°C)	$H_{m(1+2)}$ (kcal/mol)	$H_{m(1)}$ (%)	$H_{m(2)}$ (%)
DPPC		34.3	0.8	40.2	–	9.0	100	–
DPPC:OLA	100:1	32.8	0.5	–	39.9	9.0	–	100
DPPC:OLA	50:1	32.4	0.3	–	40.1	9.1	–	100
DPPC:OLA	25:1	32.6	0.2	38.9	39.9	9.2	17	83
DPPC:OLA	10:1	–	–	38.9	39.9	9.3	21	79
DPPC:OLA	5:1	–	–	40.0	40.9	9.1	32	68
DPPC:OLA	2.5:1	–	–	39.1	41.0	8.6	31	69
DPPC:OLA	1.6:1	–	–	39.1	41.4	7.0	48	52
DPPC:MSL	50:1	32.0	0.2	39.5	40.0	8.6	5	95
DPPC:MSL	25:1	31.7	0.1	39.8	40.2	8.5	23	77
DPPC:MSL	2.5:1	–	–	39.8	41.8	5.6	35	65
DPPC:URL	25:1	32.8	0.3	40.1	40.7	8.7	75	25
DPPC:URL	5:1	33.5	0.2	40.3	41.4	10.5	50	50
DPPC:URL	2.5:1	33.7	0.1	40.3	41.7	8.7	36	64
DPPC:URL	1.6:1	–	–	40.3	41.8	7.7	28	72
POPC		–	–	−5.2	–	3.2	100	–
POPC:OLA	50:1	–	–	−6.0	−5.0	3.1	7	93
POPC:OLA	25:1	–	–	−6.4	−5.1	3.3	10	90

composition. Its contribution was negligible (absorbance value at 360 nm–0.05) and no corrections were made to the polarization values [35]. At the lipid sample concentration used, the inner filter effect was not important. Fluorescence polarization was calculated according to the equation [36]:

$$P = (I_{VV} - GI_{VH}) / (I_{VV} + GI_{VH})$$

I_{vv} and I_{vh} are the fluorescence intensity values measured with the excitation and emission polarizers in parallel and perpendicular, respectively. G is the instrumental factor. All fluorescence data are mean values from three independent experiments.

3. Results

3.1. Effect of TTPs on the lipid thermotropic phase behaviour

The thermotropic behaviour of pure DPPC and POPC bilayers in the absence and presence of increasing concentrations of TTPs was analysed by DSC (Fig. 2 and Table 1). DPPC showed a lamellar gel ($L_{\beta'}$) to rippled gel ($P_{\beta'}$) phase transition (Tp = 34.3 °C and ΔH = 0.8 kcal/mol) and to lamellar liquid crystalline (L_{α}) phase transition (T_m = 40.2 °C and ΔH = 9.0 kcal/mol). The main effect of TTPs on the DSC endotherm of the DPPC membranes was a broadening and a concentration-dependent decrease in the enthalpy of the peak associated with the $L_{\beta'}$-to-$P_{\beta'}$ phase transition, while the T_p value was scarcely affected. In addition, the peak shape of $P_{\beta'}$-to-Lα phase transition was broadened revealing increased asymmetry. They induced the splitting of the main calorimetric peak into two peaks (T_{m1} and T_{m2}) and decreased the total transition enthalpy (up to 30%) at high TTP concentration. The peak decomposition analysis showed that the three compounds had a light concentration effect on the T_m values of the peak components (see Table 1). OLA and MSL, contrary to URL, increased the relative contribution of the lower T_{m1} component to the total ΔH at the expenses of the higher melting component (T_{m2}) that closely resembled the DSC endotherm of DPPC alone. TTP aggregation giving solid or crystalline precipitates was checked by DSC and phase contrast microscopy. By scanning DPPC:TTP mixtures containing different molar ratios of TTP in a temperature range of 5–97 °C, we obtained repetitive scans in the DPPC phase transitions range temperature. When we re-scanned old samples stored at −20 °C for months, some of them showed two complex endothermic peaks ~84 and 89 °C and the profile depended of the history of the sample (data not shown). A marked hysteresis between the heating and cooling polymorphic phase transitions was observed in the range temperature of 60–90 °C. These endothermic peaks could be assigned to TTP aggregates (or even crystals). In parallel with the DSC study, the phase optical microscopy showed no presence of TTP crystalline aggregate precipitation from lipid vesicles, as evidenced by the absence of needle-like TTP crystals (data not shown). However, we cannot discard the presence of micro-crystals on a scale much smaller than 1 μm due to the limited magnification power of the light microscope. Working with POPC:TTP mixtures, the L_{β}-to-L_{α} phase transition showed a profile similar to DPPC:TTP samples. Next, we studied the effect of TTPs on the thermotropic behaviour of DPPC membranes enriched with Cho. Based on experimental and simulation studies, Cho has a big effect on the properties of the lipid bilayer up to 30 mol% [37,38]. Therefore, our study was focussed on DPPC:Cho (70:30, molar ratio = 30 mol%) mixtures (Fig. 2D and Table 2). Peak decomposition analysis of DPPC:Cho melting curves indicated the existence of two peaks with Tm values close to the main-phase transition of pure DPPC. The presence of two phases could be in line with the computed-phase diagram model reported for the water–DMPC–Cho system [37], where a gel phase containing small Cho-rich

Table 2
Calorimetric data of the effect of triterpenic acids in DPPC-Cholesterol membranes. DPPC, 1,2-dipalmitoyl-*sn*-glycero-3-phosphoethanolcholine; Cho, cholesterol; OLA, oleanoic acid; URL, ursolic acid; MSL, maslinic acid. Calorimetric data are mean values of two independent experiments. T_{m1}, T_{m2} and T_{m3} are the transition temperatures of the three peaks obtained in the deconvolution analysis. H_{m1}, H_{m2} and H_{m3} are the relative areas of each peak.

Sample	Molar ratio	$T_{m(1)}$ (°C)	$T_{m(2)}$ (°C)	$T_{m(3)}$ (°C)	$H_{m(1+2+3)}$ (kcal/mol)	$H_{m(1)}$ (%)	$H_{m(2)}$ (%)	$H_{m(3)}$ (%)
DPPC:Cho	70:30	39.5	40.1	–	4.2	61	39	–
DPPC:Cho:OLA	70:30:10	39.2	39.9	41.0	4.3	25	41	34
DPPC:Cho:MSL	70:30:10	39.1	40.3	–	4.5	41	59	–
DPPC:Cho:URL	70:30:10	38.7	39.9	41.2	4.0	16	47	37

clusters, liquid ordered and liquid disordered L_α phases could be developed at a concentration of Cho 30 mol% by increasing the temperature. In the ternary mixtures DPPC:Cho plus OLA, URL or MSL, three or two components were observed with defined phase transitions and associated to the coexistence of several domains, being limited to conclude about this point from the DSC data.

3.2. Effect of TTPs on the structural membrane properties

Information on the structural properties of phospholipid-TTP mixtures was obtained by X-ray diffraction studies (Fig. 3A). DPPC and DPPC:TTP samples showed a phase sequence from gel ($L_{\beta'}$) to rippled ($P_{\beta'}$) and then to liquid crystalline lamellar (L_α) phase as the temperature increased. The diffraction pattern shown by the three compounds was qualitatively similar. The phase transition of DPPC membranes ($T_p = 37$ °C and $T_m = 43$ °C) and its structural properties ($d_{L\beta'} = 6.5$ nm, $d_{P\beta'} = 7.3$ nm and $d_{L\alpha} = 6.7$ nm) were hardly altered (~1–2 Å) by TTPs (Table 3), except for the thermotropic recovery of the bilayer stacking, which was a slow kinetic process. Comparatively, DPPC:MSL samples had an L_α phase more organized. This can be seen by the smaller full width at half the maximum of the Bragg diffraction maximum. However, DPPC:URL mixtures presented an $L_{\beta'}$ phase probably better stacked, with two diffraction orders seen relative to a single one in DPPC:MSL and not much difference in the WAXS pattern.

The main structural effect of TTPs was on the $L_{\beta'}$ and $P_{\beta'}$ phases (Fig. 4). The three compounds induced the disappearance of the $P_{\beta'}$ phase in agreement with the calorimetric study. Focusing the analysis on the thermotropic behaviour of the DPPC:OLA mixtures, OLA decreased the area (and the intensity height) of the SAXS peak associated with the $L_{\beta'}$ phase in a concentration dependent manner (Fig. 4A). However, the WAXS pattern that is associated to the lipid hydrocarbon chain order remained unaffected at all sample compositions (Fig. 4B). Noteworthy, the shape and the intensity of the peak at $s = 2.44$ nm^{-1} in the WAXS was similar in all the samples over a wide range of the DPPC:OLA ratios. These structural properties, taken together, could indicate the occurrence of local domains with some structural order (like micelles or domains with different thickness), in the gel phase of the DPPC:TTP mixtures. A similar behaviour was observed for the DPPC:URL and DPPC:MSL mixtures. In turn, the SAXS pattern associated with the L_α phase showed a profile with the same

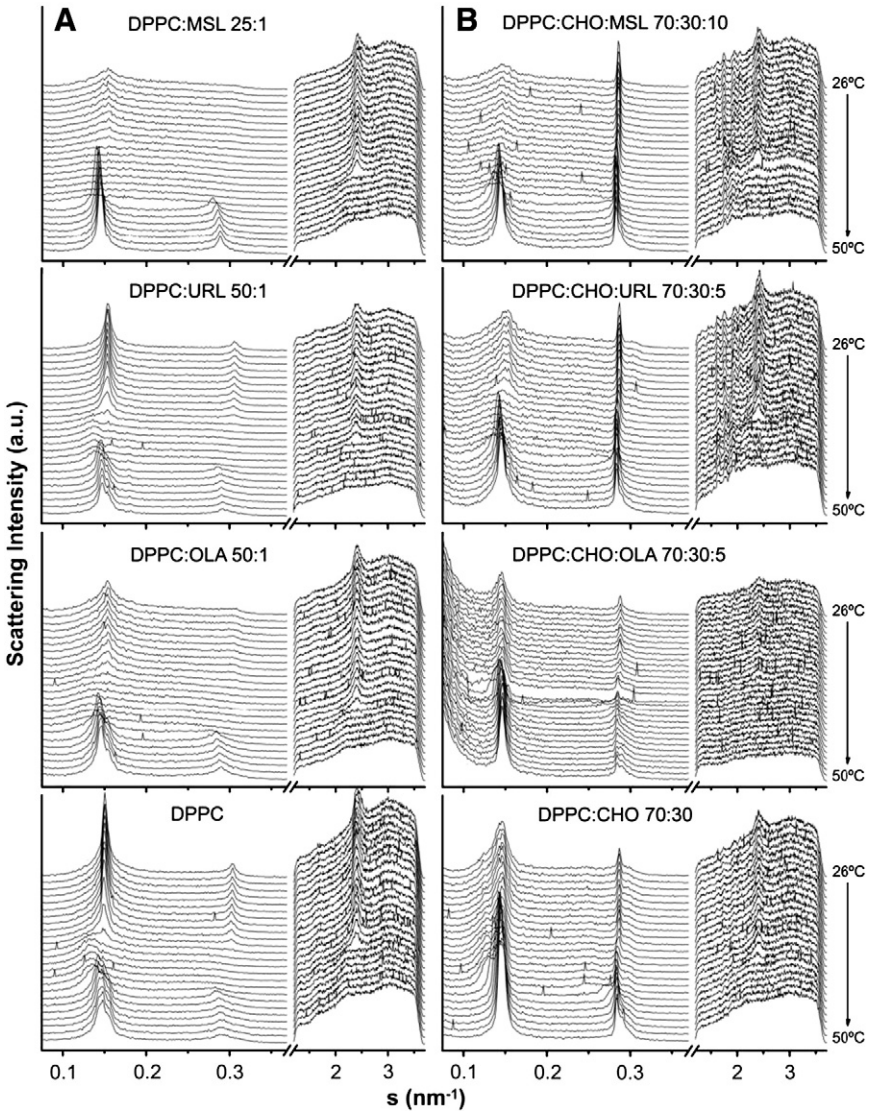

Fig. 3. Linear plots of the X-ray scattering patterns. (A) DPPC:TTP and (B) DPPC:Cho:TTP mixtures at the molar ratio specified. The sequence of the patterns was acquired under kinetic conditions with a scan rate of 1 °C/min. Successive diffraction patterns were collected for 15 s each minute. The $L_{\beta'}$ phase was identified by the two peaks of reflections in the SAXS ($s \approx 0.150$ nm^{-1}), accompanied by a clear reflection in the WAXS region. The $P_{\beta'}$ phase was recognized by the well-defined reflection in the WAXS region, accompanied by a SAXS broad reflection ($s \approx 0.135$ nm^{-1}). The L_α phase was known by the two peaks of reflection in the SAXS and the absence of the diffraction peak in the WAXS. The $P_{\beta'}$-to-L_α phase transition was identified by the vanishing peak in the WAXS region of the pattern. Only the heating sequence from 25 °C to 50 °C is shown.

Table 3
Structural properties of DPPC-triterpene membranes. DPPC, 1,2-dipalmitoyl-*sn*-glycero-3-phosphoethanolcholine; POPC, 1-palmitoyl-2-oleoyl-*sn*-glycero-3-phosphocholine; Cho, cholesterol; OLA, oleanolic acid; URL, ursolic acid; MSL, maslinic acid. Repeat distance, $d_{L\beta'}$ at 30°C, $d_{P\beta'}$ at 40°C and $d_{L\alpha}$ at 48°C and 40°C for DPPC and POPC membranes, respectively.

Sample	Molar ratio	$d_{L\beta'}$ (nm)	$d_{P\beta'}$ (nm)	$d_{L\alpha}$ (nm)
DPPC	–	6.62	7.30	6.72
DPPC:OLA	100:1	6.45	6.85	6.66
DPPC:OLA	50:1	6.45	7.20	6.84
DPPC:OLA	40:1	6.45	–	6.90
DPPC:OLA	25:1	6.39	6.90	6.74
DPPC:OLA	20:1	6.37	–	6.95
DPPC:OLA	10:1	6.56	–	6.92
DPPC:OLA	2.5:1	6.43	–	6.87
DPPC:URL	50:1	6.49	7.26	6.74
DPPC:URL	25:1	6.61	7.32	6.83
DPPC:URL	2.5:1	6.52	–	7.17
DPPC:MSL	50:1	6.44	7.10	6.87
DPPC:MSL	25:1	6.43	–	6.87
DPPC:Cho	70:30	7.09	7.89	6.85
DPPC:Cho:OLA	70:30:5	6.84	6.86	6.90
DPPC:Cho:URL	70:30:5	6.82	7.22	6.91
DPPC:Cho:MSL	70:30:10	6.83	7.02	6.91
POPC	–			6.46
POPC:OLA	50:1			6.46
POPC:OLA	25:1			6.54
POPC:OLA	5:1			6.86

characteristics regarding the changes of the TTP concentration (see Fig. 3). TTPs affected the organization of the lamellar stacking of the DPPC bilayers and reduced the SAXS peak area related to the L_α at high concentrations. We also analysed the thermotropic behaviour of the POPC:OLA and DEPE:OLA mixtures. OLA altered the diffraction pattern of the POPC membranes (L_α phase with d = 6.46 nm at 40 °C) in a similar form as the DPPC bilayers in the L_α phase. On the other hand, the phase transitions of DEPE from L_β-to-L_α (Tm = 38 °C) and then to H_{II} phases (T_H = 66 °C) and its structural properties ($d_{L\beta}$ = 6.59 nm, $d_{L\alpha}$ = 5.55 nm and d_{HII} = 6.40 nm) were hardly changed by the presence of TTPs (data not shown).

3.2.1. Lipid mixture DPPC:Cho

X-ray diffraction analysis of DPPC:Cho (70:30 M ratio) in the presence and absence of TTPs were done (Fig. 3B). DPPC:Cho mixtures showed the coexistence of $L_{\beta'}$ and $P_{\beta'}$ phases from 25 °C until the L_α phase transition (T_m = 44 °C) was observed. Structural aggregates of Cho were also detected (notice a constant peak at 3.5 nm and small crystalline peaks in the WAXS region). MSL and URL altered the diffraction pattern of the DPPC:Cho rich membranes inducing the appearance of the defined peaks in the WAXS region indicating the presence of domains with the structural order (possibly aggregates or domains with different thicknesses), and increasing the intensity peak at 3.5 nm appointing to the segregation of Cho from the bilayer in its presence. On the contrary, OLA showed a diffraction pattern corresponding to a matrix poorly ordered accompanied by a decrease in the intensity peak at 3.5 nm.

3.3. ^{31}P-NMR data

The presence of the structural domains in the DPPC:TTP mixtures, indicated by the X-ray diffraction analysis, was studied by ^{31}P NMR spectroscopy (Fig. 5). The DPPC spectra showed line shapes characteristic of gel and L_α phases (data not shown) in agreement with data published [39]. The ^{31}P NMR spectra of DPPC:URL mixtures (50:1 and 25:1 M ratio) proved the coexistence of different structures in function of the temperature. At 30 °C, DPPC:URL samples showed an asymmetric line shape with a low-field shoulder and a high-field peak, indicative of a gel phase. At 42 °C, the spectra of an L_α phase was

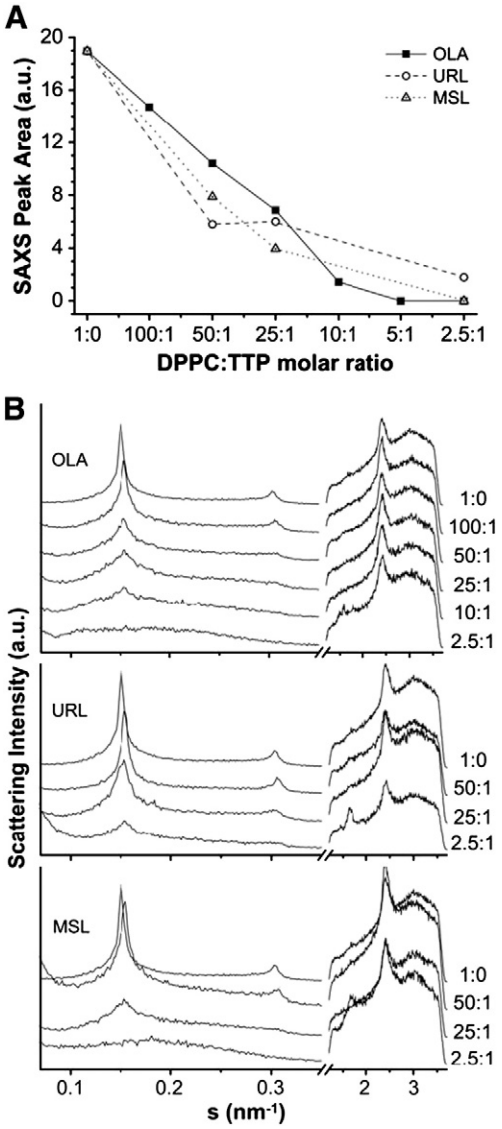

Fig. 4. Analysis of the X-ray scattering pattern of DPPC:TTP samples. (A) SAXS peak area associated with the $L_{\beta'}$ phase in function of DPPC:TTP molar ratio. (B) X-ray diffraction pattern of DPPC:TTP mixtures at the molar ratio indicated. The study was conducted at 26 °C.

superimposed by a symmetrical signal corresponding to a fast isotropic motion of the lipid molecules, centered at around 0 ppm, that became slightly more defined by increasing the temperature (up

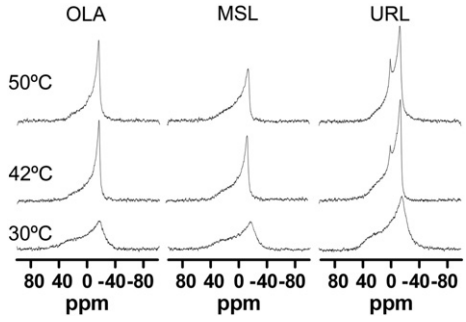

Fig. 5. ^{31}P NMR spectra of DPPC-triterpene membranes. Spectra for selected temperatures of DPPC:OLA, DPPC:MSL and DPPC:URL mixtures at 25:1 M ratio. Samples were equilibrated 15 min at each temperature before obtaining the spectra by scanning from a lower to a higher temperature.

to 55 °C). In contrast, the DPPC:OLA and DPPC:MSL samples showed no isotropic signal and the ^{31}P NMR spectra were similar to that observed for the DPPC membranes. On the other hand, the ^{31}P NMR spectra of DPPC-Cho (30 mol%) in the absence and in the presence of TTPs was virtually identical and exhibited the shape and basal linewidth (~90 ppm) characteristic of a liquid crystalline phase and the absence of any isotropic peak (data not shown).

3.4. Steady-state fluorescence study

We examined if TTPs affect the phase properties of DPPC and DPPC-Cho membranes. For this purpose, we measured the fluorescence properties of Laurdan, a sensitive probe to changes in polarity at the membrane–water interface [40,41]. The Laurdan emission generalised polarization (GP) values as a function of temperature, which were calculated in pure DPPC and DPPC-Cho (30 mol%) membranes in the absence and in the presence of TTPs (Fig. 6). In the DPPC membranes, the GP value decreased from ~0.5 in the gel phase to ~−0.2 for the liquid crystalline phase. The melting temperature was in the range of 40–45 °C, in agreement with the DSC data. TTPs hardly changed the Laurdan emission shift ~2–3 nm at 25 and 50 °C, with no differences between them. GP values were scarcely altered in both phases, suggesting a minor effect of TTPs on the DPPC phase polarity. In the DPPC-Cho (30 mol%) membranes, the Laurdan emission spectra had a blue shift in the presence of TTPs, evident in the liquid crystalline phase. The spectra seem to indicate a mixture of environments of Laurdan when TTPs are present. The temperature interval of the phase transition was broader and shifted at a higher temperature in the presence of TTPs. The three compounds showed a similar GP/temperature profile, increasing the GP values at temperatures above 40 °C.

The fluorescence polarization of the probe DPH was also used to further investigate the effect of OLA, MSL and URL on the lipid environment in deep regions of the DPPC membranes. The hydrophobic probe DPH is located into the membrane palisade [42] and its fluorescence polarization changes are related to an altered molecular order of the hydrophobic membrane region. The fluorescence polarization of DPH-labeled DPPC liposomes in the absence and presence of the three TTPs had the same trend with an apparent gel-to-liquid crystalline transition temperature ~41–43 °C and a phase transition amplitude of ~73% for DPPC alone and ~65–69% in the presence of TTPs, in the range of 80:1 to 20:1 DPPC:TTP molar ratio (data not shown). None of the three compounds had an important effect on the polarization values above the phospholipid phase transition.

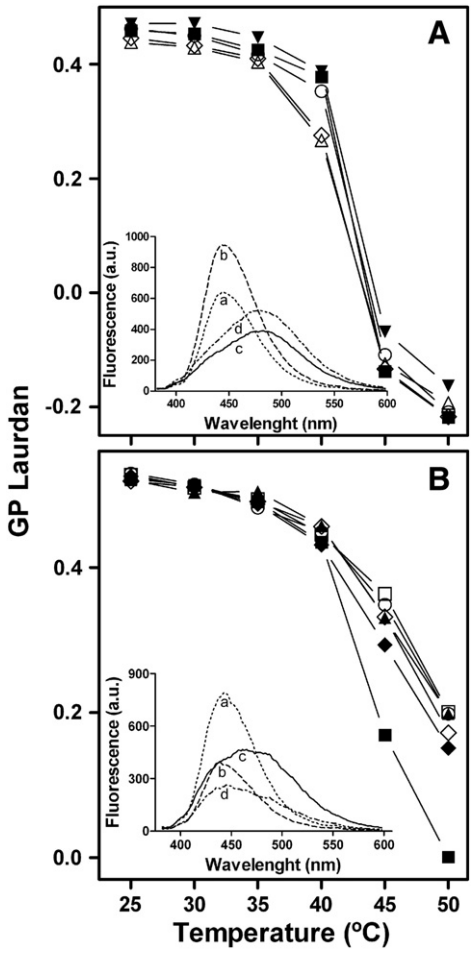

Fig. 6. Effect of triterpenic acids on the temperature dependence of Laurdan emission GP values in DPPC and DPPC:Cho membranes. (A) DPPC membranes in absence (■) and in presence of TTPs at the molar ratio DPPC:TTP of OLA 100 (Δ) and 25 (▼), MSL 25 (◊) and URL 25 (o). Insert: Laurdan fluorescence spectra of DPPC membranes in absence (a, c) and presence of OLA (25:1, molar ratio) (b, d) recorded at 25 (a, b) and 50 °C (c, d). (B) DPPC:Cho 30 mol% membranes in absence (■) and presence of TTPs at the molar ratio DPPC:TTP of OLA 50 (□), MSL 50 (▲), MSL 25 (◊), URL 50 (◆) and URL 25 (O). Insert: Laurdan fluorescence spectra of DPPC:Cho membranes in absence (a, c) and in presence of OLA (50:1, molar ratio) (b, d) recorded at 25 (a, b) and 50 °C (c, d).

4. Discussion

A clear understanding of the molecular mechanisms of action of TTPs is crucial in the valuation of these molecules as nutriceutical compounds with potential preventive and therapeutic properties. The structural characteristics of OLA, MSL and URL suggest that the three compounds should be able to interact with the cell membranes thereby modulating the cell membrane structure. Thus, an important part of the molecular mechanism underlying the diverse biological activities of TTPs could be related to the TTP–membrane interaction. Our study provides experimental evidence that OLA, MSL and URL alter the structural properties of the PC and PC-Cho rich membranes with subtle differences in the membrane effects depending on the TTP chemical structure.

TTPs in lipid membranes form complex systems with nonideal behaviour. The calorimetric study showed that the three compounds abolished the DPPC pre-transition and did not affect significantly the melting temperature and the enthalpy of the main phase transition. These observations indicate that TTPs are located close to the lipid head groups in the bilayer interface [43]. The thermotropic behaviour of the DPPC:TTP samples was characteristic of a non-homogeneous mixture with the TTP phase segregation and the formation of DPPC-TTP rich and -TTP poor domains. TTPs showed subtle differences in the phase segregation features related to their chemical structure. For example, in the peak decomposition of the main phase transition, OLA and MSL (a hydroxyl-derivative of OLA) increased the relative area of the low melting peak in a concentration-dependent manner, while URL acted in the opposite way. The X-ray diffraction analysis allows us to conclude that TTPs alter the structural order of the $L_{\beta'}$ phase without destabilizing the lipid bilayer to any significant extent. The transition $L_{\beta'}$-to-$P_{\beta'}$ phase and the $P_{\beta'}$ phase disappeared in function of the TTP concentration, due to an effect of TTPs on the tilted all-trans conformation of the PL acyl-chains, in agreement with the calorimetric data. The SAXS and WAXS diffraction patterns in the gel phase showed the appearance of the structural entities that could be due to the self-assembly of lipids in the DPPC:TTP rich domains. From considerations of the WAXS pattern, these units seem to have a structure that looks like poorly organized micelles (especially in the DPPC-OLA and -MSL systems). The presence of a nonbilayer isotropic phase superimposed in the liquid crystalline L_{α} phase in the DPPC:URL samples, observed in ^{31}P NMR spectra, demonstrated the existence of the lipid structures with high curvature (probably inverted micelles) in the membrane.

It has been reported that the TTP compounds have limited solubility in the DPPC membranes [31,44]. In particular, the

concentration of the URL incorporation within the DPPC liposomes has been quantified to be ~5% molar ratio working with the DPPC:URL (10:1 M ratio) mixtures (~50% of the theoretical value) [44]. From the consideration of the solubility data reported for several TTP compounds, we could assume that the limit of TTPs miscibility in the DPPC membranes might be around 20:1 lipid:TTP molar ratio. The partial miscibility of TTPs in the phospholipid membrane could support the appearance of the phase segregation features shown in the DSC study. In particular, the isotropic peak observed in the NMR experiments with the DPPC:URL mixtures that correlates with the prominent double peak in the DSC thermogram could represent a general property of the TTPs under study to induce phase segregation and micellarization effects in the PC membranes. TTP exclusion from the bilayer and its existence as a solid precipitate cannot be excluded from considerations of the DSC assays. The DPPC:TTP systems seem to be a multiphasic system including a TTP solid phase and a DPPC:TTP phase. If and to what degree the TTP membrane effects take place will depend on the pH, the structure of each particular TTP and the phospholipid system. TTPs have pK values in solution around 5.0 [45]. However, the apparent pK values of the free fatty acids in a lipid membrane environment are close to the physiological pH 7.4 used to conduct the experiments [46]. Thus, the complex membrane effects observed for each particular TTP would also be affected by the pH-dependent combined effects of the protonated and deprotonated forms with different tendencies to micellarize and/or associate with the membrane lipids. OLA and URL are structurally similar congeners, therefore some structural features like the methyl group position in the E-ring in the pentacyclic backbone could influence the location of the pentacyclic moiety within the lipid bilayer and its effect on the phase segregation (or domains formation) features.

The membrane phase properties induced by Cho are sensitive to the TTP-interaction as underlined by their differential effect on the biophysical properties of the DPPC and DPPC:Cho rich membranes. The X-ray diffraction study proved that MSL and URL caused the appearance of domains with the structural order in the DPPC:Cho membranes and the segregation of Cho from the bilayer. In contrast, OLA reduced the structural organization of the Cho-rich membranes. These results are in line with the DSC study proving the presence of the membrane domains and a lack of specific TTP–Cho interactions. The Laurdan fluorescence spectra in the presence of TTPs also indicated the presence of the co-existing domains with diverse polar environments. The increase in the Laurdan GP values above 40 °C, which is a general characteristic of TTPs, might be associated to changes in the liquid-ordered phases in coexistence with the liquid disordered phases. Differences in the TTP effects in the DPPC:Cho membranes must be related to the structural properties of each particular compound. OLA and URL are position isomers and MSL is the 2-hydroxyderivative of OLA. The chemical arrangement of the 2β-hydroxy group in the A-ring in MSL and the methyl groups in the E-ring in URL, compared to OLA, could play a major role in determining the local position of the TTP molecule in the interfacial region in the lipid bilayer and its effect on the lateral organization of the Cho-rich membrane domains. Possibly, URL and MSL would partition into DPPC:Cho domains and compete with Cho for the hydrogen-bonded ester carbonyl groups, disturbing the presence of the Cho-rich domains. In turn, OLA could have a deeper penetration in the membranes thereby influencing the membrane fluidity and disturbing the presence of the liquid ordered Cho-rich domains. The degree of permeation of each TTP molecule into the bilayer would be a compromise between the number of hydrophobic contacts and the cost of loosing some H-bonds with water. Therefore, the membrane lipid composition would also influence the relative position of each TTP in the bilayer. This point deserves to be scrutinized in a future study.

TTPs share structural similarities with sterols, which are the major building blocks of "raft-like" platforms or segregated membrane domains that in turn play an important role in the cell signalling processes. Our results with synthetic model membranes suggest that the studied TTPs are able to perturb such Cho-enriched membrane domains and therefore are likely to affect the lateral domain heterogeneity of the cell membranes. This circumstance confers a certain capacity to TTPs to influence also localization and, hence, physiological function of the membrane-associated proteins related to such domains. It is probable that some of the distinct biological effects described for the TTPs may be partially attributable to their ability to interact with the Cho-rich membrane domains and to induce changes in membrane lateral heterogeneity thereby affecting pivotal cellular signal transduction pathways. Although the present data were obtained with model lipid systems and require further investigation to link concrete TTP effects on the cell membrane structure to specific cell biological results, they already strongly suggest a membrane-related mechanism as a mode of action regarding their biological activity. TTP interactions with the cell membrane must be considered to understand the molecular basis underlying their biological effects.

Acknowledgements

This research has received funding from the European Community's Seventh Framework Programme (FP7/2007–2013): DESY-HASYLAB-Project No. II-20090005 EC, "Comision Interministerial de Ciencia y Tecnología" (CICYT, AGL2008-02258) and "Instituto de Salud Carlos III" (RD06/0045). The triterpene 2α-hydroxyoleanoic acid (maslinic acid) was kindly provided by Dra. A. Guinda (Instituto de la Grasa, CSIC-Sevilla, Spain).

References

[1] J. Liu, Oleanolic acid and ursolic acid: research perspectives, J. Ethnopharmacol. 100 (2005) 92–94.
[2] M.D. Herrera, R. Rodriguez-Rodriguez, V. Ruiz-Gutierrez, Functional properties of pentacyclic triterpenes contained in "Orujo" olive oil, Curr. Nutr. Food Sci. 2 (2006) 45–49.
[3] M.C. Perez-Camino, A. Cert, Quantitative determination of hydroxy pentacyclic triterpene acids in vegetable oils, J. Agric. Food Chem. 47 (1999) 1558–1562.
[4] C. Romero, A. García, E. Medina, M.V. Ruíz-Méndez, A.D. Castro, M. Brenes, Triterpenic acids in table olives, Food Chem. 118 (2010) 670–674.
[5] H. Safayhi, E.R. Sailer, Anti-inflammatory actions of pentacyclic triterpenes, Planta Med. 63 (1997) 487–493.
[6] M.P. Montilla, A. Agil, M.C. Navarro, M.I. Jimenez, A. Garcia-Granados, A. Parra, M.M. Cabo, Antioxidant activity of maslinic acid, a triterpene derivative obtained from Olea europaea, Planta Med. 69 (2003) 472–474.
[7] R. Rodriguez-Rodriguez, E. Stankevicius, M.D. Herrera, L. Ostergaard, M.R. Andersen, V. Ruiz-Gutierrez, U. Simonsen, Oleanolic acid induces relaxation and calcium-independent release of endothelium-derived nitric oxide, Br. J. Pharmacol. 155 (2008) 535–546.
[8] S.J. Tsai, M.C. Yin, Antioxidative and anti-inflammatory protection of oleanolic acid and ursolic acid in PC12 cells, J. Food Sci. 73 (2008) H174–H178.
[9] T.J. Raphael, G. Kuttan, Effect of naturally occurring triterpenoids ursolic acid and glycyrrhizic acid on the cell-mediated immune responses of metastatic tumor-bearing animals, Immunopharmacol. Immunotoxicol. 30 (2008) 243–255.
[10] L.O. Somova, A. Nadar, P. Rammanan, F.O. Shode, Cardiovascular, antihyperlipidemic and antioxidant effects of oleanolic and ursolic acids in experimental hypertension, Phytomedicine 10 (2003) 115–121.
[11] R. Rodriguez-Rodriguez, M.D. Herrera, J.S. Perona, V. Ruiz-Gutierrez, Potential vasorelaxant effects of oleanolic acid and erythrodiol, two triterpenoids contained in 'orujo' olive oil, on rat aorta, Br. J. Nutr. 92 (2004) 635–642.
[12] R. Rodriguez-Rodriguez, J.S. Perona, M.D. Herrera, V. Ruiz-Gutierrez, Triterpenic compounds from "orujo" olive oil elicit vasorelaxation in aorta from spontaneously hypertensive rats, J. Agric. Food Chem. 54 (2006) 2096–2102.
[13] R. Rodriguez-Rodriguez, M.D. Herrera, M.A. de Sotomayor, V. Ruiz-Gutierrez, Pomace olive oil improves endothelial function in spontaneously hypertensive rats by increasing endothelial nitric oxide synthase expression, Am. J. Hypertens. 20 (2007) 728–734.
[14] J. Liu, H. Sun, X. Wang, D. Mu, H. Liao, L. Zhang, Effects of oleanolic acid and maslinic acid on hyperlipidemia, Drug Dev. Res. 68 (2007) 261–266.
[15] H.X. Xu, F.Q. Zeng, M. Wan, K.Y. Sim, Anti-HIV triterpene acids from Geum japonicum, J. Nat. Prod. 59 (1996) 643–645.
[16] C.M. Struch, S. Jaeger, C.M. Schempp, A. Scheffler, S.F. Martin, Solubilized triterpenes from mistletoe show anti-tumor effects on skin-derived cell lines, Planta Med. 74 (2008) 1130.
[17] R. Martin, J. Carvalho-Tavares, E. Ibeas, M. Hernandez, V. Ruiz-Gutierrez, M.L. Nieto, Acidic triterpenes compromise growth and survival of astrocytoma cell

lines by regulating reactive oxygen species accumulation, Cancer Res. 67 (2007) 3741–3751.
[18] F.J. Reyes, J.J. Centelles, J.A. Lupianez, M. Cascante, (2Alpha, 3beta)-2, 3-dihydroxyolean-12-en-28-oic acid, a new natural triterpene from *Olea europea*, induces caspase dependent apoptosis selectively in colon adenocarcinoma cells, FEBS Lett. 580 (2006) 6302–6310.
[19] F.J. Reyes-Zurita, E.E. Rufino-Palomares, J.A. Lupianez, M. Cascante, Maslinic acid, a natural triterpene from *Olea europaea* L., induces apoptosis in HT29 human colon-cancer cells via the mitochondrial apoptotic pathway, Cancer Lett. 273 (2009) 44–54.
[20] M.E. Juan, J.M. Planas, V. Ruiz-Gutierrez, H. Daniel, U. Wenzel, Antiproliferative and apoptosis-inducing effects of maslinic and oleanolic acids, two pentacyclic triterpenes from olives, on HT-29 colon cancer cells, Br. J. Nutr. 100 (2008) 36–43.
[21] J. Fernandes, R.O. Castilho, M.R. da Costa, K. Wagner-Souza, M.A. Coelho Kaplan, C. R. Gattass, Pentacyclic triterpenes from Chrysobalanaceae species: cytotoxicity on multidrug resistant and sensitive leukemia cell lines, Cancer Lett. 190 (2003) 165–169.
[22] A. Marquez Martin, R. de la Puerta Vazquez, A. Fernandez-Arche, V. Ruiz-Gutierrez, Supressive effect of maslinic acid from pomace olive oil on oxidative stress and cytokine production in stimulated murine macrophages, Free Radic. Res. 40 (2006) 295–302.
[23] W. Zou, X. Liu, P. Yue, Z. Zhou, M.B. Sporn, R. Lotan, F.R. Khuri, S.Y. Sun, c-Jun NH2-terminal kinase-mediated up-regulation of death receptor 5 contributes to induction of apoptosis by the novel synthetic triterpenoid methyl-2-cyano-3, 12-dioxooleana-1, 9-dien-28-oate in human lung cancer cells, Cancer Res. 64 (2004) 7570–7578.
[24] C. Genet, A. Strehle, C. Schmidt, G. Boudjelal, A. Lobstein, K. Schoonjans, M. Souchet, J. Auwerx, R. Saladin, A. Wagner, Structure–activity relationship study of betulinic acid, a novel and selective TGR5 agonist, and its synthetic derivatives: potential impact in diabetes, J. Med. Chem. 53 (2010) 178–190.
[25] T. Maruyama, K. Tanaka, J. Suzuki, H. Miyoshi, N. Harada, T. Nakamura, Y. Miyamoto, A. Kanatani, Y. Tamai, Targeted disruption of G protein-coupled bile acid receptor 1 (Gpbar1/M-Bar) in mice, J. Endocrinol. 191 (2006) 197–205.
[26] K.F. Ferri, G. Kroemer, Organelle-specific initiation of cell death pathways, Nat. Cell Biol. 3 (2001) E255–E263.
[27] J. Henry-Mowatt, C. Dive, J.C. Martinou, D. James, Role of mitochondrial membrane permeabilization in apoptosis and cancer, Oncogene 23 (2004) 2850–2860.
[28] S.W. de Laat, P.T. van der Saag, S.A. Nelemans, M. Shinitzky, Microviscosity changes during differentiation of neuroblastoma cells, Biochim. Biophys. Acta 509 (1978) 188–193.
[29] H. Hachisuka, H. Nomura, O. Mori, S. Nakano, K. Okubo, M. Kusuhara, M. Karashima, E. Tanikawa, M. Higuchi, Y. Sasai, Alterations in membrane fluidity during keratinocyte differentiation measured by fluorescence polarization, Cell Tissue Res. 260 (1990) 207–210.
[30] S.K. Han, Y.I. Ko, S.J. Park, I.J. Jin, Y.M. Kim, Oleanolic acid and ursolic acid stabilize liposomal membranes, Lipids 32 (1997) 769–773.
[31] S. Rodríguez, H.A. Garda, H. Heinzen, P. Moyna, Effect of plant monofunctional pentacyclic triterpenes on the dynamic and structural properties of dipalmitoyl-phosphatidylcholine bilayers, Chem. Phys. Lipids 89 (1997) 119–130.
[32] M. Hu, K. Konoki, K. Tachibana, Cholesterol-independent membrane disruption caused by triterpenoid saponins, Biochim. Biophys. Acta 1299 (1996) 252–258.
[33] S.S. Funari, F. Barcelo, P.V. Escriba, Effects of oleic acid and its congeners, elaidic and stearic acids, on the structural properties of phosphatidylethanolamine membranes, J. Lipid Res. 44 (2003) 567–575.
[34] T. Parasassi, G. De Stasio, G. Ravagnan, R.M. Rusch, E. Gratton, Quantitation of lipid phases in phospholipid vesicles by the generalized polarization of Laurdan fluorescence, Biophys. J. 60 (1991) 179–189.
[35] B.R. Lentz, B.M. Moore, D.A. Barrow, Light-scattering effects in the measurement of membrane microviscosity with diphenylhexatriene, Biophys J. 25 (1979) 489–494.
[36] J.R. Lakowicz, Fluorescence anisotropy, in: J.R. Lakowicz (Ed.), Principles of Fluorescente Spectroscopy, Springer Science, New York, 2006, pp. 355–381.
[37] F. de Meyer, B. Smit, Effect of cholesterol on the structure of a phospholipid bilayer, Proc. Natl. Acad. Sci. USA 106 (2009) 3654–3658.
[38] W.C. Hung, M.T. Lee, F.Y. Chen, H.W. Huang, The condensing effect of cholesterol in lipid bilayers, Biophys. J. 92 (2007) 3960–3967.
[39] P.R. Cullis, B. de Kruijff, Lipid polymorphism and the functional roles of lipids in biological membranes, Biochim. Biophys. Acta 559 (1979) 399–420.
[40] T. Parasassi, M. Di Stefano, M. Loiero, G. Ravagnan, E. Gratton, Cholesterol modifies water concentration and dynamics in phospholipid bilayers: a fluorescence study using Laurdan probe, Biophys. J. 66 (1994) 763–768.
[41] T. Parasassi, E.K. Krasnowska, L. Bagatolli, E. Gratton, Laurdan and prodan as polarity-sensitive fluorescent membrane probes, J. Fluoresc. 8 (1998) 365–373.
[42] R.D. Kaiser, E. London, Location of diphenylhexatriene (DPH) and its derivatives within membranes: comparison of different fluorescence quenching analyses of membrane depth, Biochemistry 37 (1998) 8180–8190.
[43] T. Heimburg, A model for the lipid pretransition: coupling of ripple formation with the chain-melting transition, Biophys. J. 78 (2000) 1154–1165.
[44] S. Rodriguez, M.V. Cesio, H. Heinzen, P. Moyna, Determination of the phospho-lipid/lipophilic compounds ratio in liposomes by thin-layer chromatography scanning densitometry, Lipids 35 (2000) 1033–1036.
[45] B. Claude, P. Morin, M. Lafosse, P. Andre, Evaluation of apparent formation constants of pentacyclic triterpene acids complexes with derivatized beta- and gamma-cyclodextrins by reversed phase liquid chromatography, J. Chromatogr. A 1049 (2004) 37–42.
[46] D.M. Small, D.J. Cabral, D.P. Cistola, J.S. Parks, J.A. Hamilton, The ionization behavior of fatty acids and bile acids in micelles and membranes, Hepatology 4 (1984) 77S–79S.